ELSEVIER

Computer Methods and Programs in Biomedicine 68 (2002) 37–47

Computer Methods and Programs in Biomedicine

www.elsevier.com/locate/cmpb

Coupling patterns between spontaneous rhythms and respiration in cardiovascular variability signals

F. Censi [a,*], G. Calcagnini [b], S. Cerutti [c]

[a] *Department of Computer and System Sciences, University of Rome 'La Sapienza' Via Nino Martoglio 5, 00137 Rome, Italy*
[b] *Biomedical Engineering Laboratory, Istituto Superiore di Sanità, Viale Regina Elena 299, 00161 Rome, Italy*
[c] *Department of Biomedical Engineering, Polytechnic University of Milan, Piazza Leonardo da Vinci, 32-20133 Milan, Italy*

Received 16 November 2000; received in revised form 5 February 2001; accepted 23 February 2001

Abstract

We performed a quantitative study of coupling patterns between respiration and spontaneous rhythms of heart rate and blood pressure variability signals by using the Recurrence Quantification Analysis (RQA). We applied RQA to both simulated and experimental data obtained in control breathing at three different frequencies (0.25, 0.20, and 0.13 Hz) from ten normal subjects. RQA succeeded in quantifying different degrees of non-linear coupling associated to several interference patterns. We found higher degrees of non-linear coupling when the respiratory frequency was close to the spontaneous Low Frequency (LF) rhythm (0.13 Hz), or almost twice the LF frequency (0.2 Hz), whereas weaker coupling was observed when the respiratory frequency was 0.25 Hz. Clinical applications of our approach should focus on new experimental protocols, featuring the stimulation of one of the two branches of the autonomic nervous system (ANS) or aimed at the analysis of pathologies linked to the ANS.

Keywords: Non-linear coupling; Cardiorespiratory synchronization; Recurrence quantification analysis; Autonomic nervous system

1. Introduction

The study of the oscillations in physiological systems and of the interactions between different oscillating sources has gained increasing attention over the last 20 years [1–3]. In particular, the quantification of specific rhythms in short-term heart rate (HR) and blood pressure (BP) variability signals has been successfully used to investigate the autonomic nervous system (ANS) control processes [4–6]. The importance of this analysis has been increased with its use in clinical diagnosis of states of diseases. In this context, the most widely used method has been spectral analysis. Using this approach, two main spectral components have been found in both HR and BP variability signals, a Low Frequency component (LF, around 0.1 Hz) probably due to the baroreflex control loop and a High Frequency component (HF, 0.18–0.4 Hz) synchronous with respiration and marker of parasympathetic activity.

* Corresponding author. Tel.: +39-06-87133633; fax: +39-06-44585367.
E-mail address: censi@dis.uniromal.it (F. Censi).

0169-2607/02/$ - see front matter
PII: S0169-2607(01)00158-4

In spite of the reliability of the power spectral analysis in estimating the harmonic contents of signals, this analysis can not be used to investigate non-linear interactions among different oscillating components. Further limitations of spectral analysis are stationarity constraints, which strongly affect spectral resolution, and the blindness to the phase information of signals. Evidences of transient non-linear interaction phenomena between respiration and cardiovascular variability signals collected so far by several studies [7–14] have been attributed to the complex dynamics involving cardiovascular control. Thus, a deeper analysis based on different signal processing techniques is needed.

In 1994, Porta et al. proposed a qualitative approach to detect and visualize non-linear interactions between LF and HF rhythms at fiber level (i.e. in the beat-to-beat variability series of sympathetic activity) [8]. In this study they used several graphical tools, including a new application of the recurrence plot (RP). The RP analysis has been originally conceived to investigate the dynamic of a system by identifying the time correlations of a single embedded time series [15]. This technique was then enhanced by the introduction of several variables to quantify the RP features [16]. However, the classical application of the RP provides qualitative and quantitative information about the dynamical structure of only one single time series. In addition this traditional approach is based on a dynamical representation of the system, thus implying the construction of a state vector using lagged values of a measured state variable.

Porta et al. proposed a new application of the RP, based on a mere comparison of the periodicity of two (state) variables in the time domain [8]. They applied the RPs to observe whether repetitive patterns characterized the interaction between two series, and showed the performances of this tool in qualitatively detecting phase-locking patterns and quasi-periodic behaviors [8,17]. However, the use of the RP to quantify non-linear interference phenomena has not been widely addressed.

The aim of this paper is to quantify the degree of non-linear coupling between respiration and spontaneous rhythms of both HR and BP variability signals by using the RP quantification approach. Since a RP portrays the dynamics of the coupling in the form of dots, its quantification provides information about the deterministic structure and the complexity of the dynamics itself.

2. Methods and materials

2.1. Data acquisition and experimental protocol

In order to analyze the interference between HR variability (HRV), BP variability (BPV) and respiration, we simultaneously recorded ECG, Arterial Blood Pressure (ABP) and Respiratory Activity (RA). Surface ECO (II lead) was recorded by an analog electrocardiograph (MCR I, Esaote, Italy). APB was continuously and non-invasively recorded by photopletismographic technique (Finapres, Omheda, USA), and RA was monitored using an estensimetric thoracic belt. The signals were sampled in real-time (sampling frequency: 500 Hz, resolution: 12 bit, DT28O1A, Data Translation, USA) and stored in a magneto-optical disk for further analysis.

Ten healthy subjects were analyzed (five males, age ranging from 25 to 28 years). Data were collected in the Clinical Pathophysiology Unit of the University of Rome 'La Sapienza'. The protocol consisted of three different stages, with the subject in paced breathing at various rates, lying supine in rest. Each stage lasted 8 min, followed by a 3-min recovery period to allow periodic calibration of the Finapres. Subjects were instructed to initiate a breath with each tone of a series of auditory cues generated by a computer. Subjects were allowed to adjust their tidal volume to a comfortable level to preserve normal ventilation. The selected breathing rates were 15, 12, and 8 breaths per min corresponding to 0.25, 0.20 and 0.13 Hz, respectively, in order to have the HF component getting progressively closer to the spontaneous LF frequency (usually around 0.1 Hz).

Signal pre-processing included the detection of QRS complexes (derivative + threshold algorithm)

[18], low-pass filtering of ABP and RA signals (FIR, filter order 10, cut-off frequency 0.5 Hz), and resampling at 2 Hz. We used the low-pass filtering of the event series to extract the HRV signals as described in [19]. This approach particularly guarantees the time synchronization between HRV, BPV and RA. Very low frequency component and low trends of HR and BP variability signals have been filtered out by highpass linear-phase filter (FIR, filter order 16, cut-off frequency 0.03 Hz).

2.2. Recurrence Quantification Analysis (RQA)

Given two time-series, $x(t)$ and $y(t)$, RP is a representation of the normalized distance between the points $(x(i), y(i))$ and $(x(j), y(j))$, plotted in the time-to-time domain. The normalized distance is obtained as follow:

$$D(i,j) = \sqrt{\frac{[x(i)-x(j)]^2}{\mathrm{var}(x)} + \frac{[y(i)-y(j)]^2}{\mathrm{var}(y)}} \qquad (1)$$

where var(·) addresses the signal variance. If $D(i, j)$ is lower than a threshold value, the point (i, j) is plotted. We set the distance threshold at 15% of the maximum distance value, computed as the 95th percentile [16].

Since the distance between a point and itself is zero ($D(i,i) = 0$), the main diagonal line in the plot is always visible. Moreover the plot is symmetric, since $D(i,j) = D(j,i)$ according to the definition of distance given in Eq. (1).

A recurrent point in (i,j) means that the interaction between the signals in the instant i is almost the same as in the instant j, i.e. the interaction is recurring. Particularly, a spurious recurrent point indicates an isolated recurrence of the phase relationship between the signals, either by accident/noise or by a true interaction. Line segments parallel to the main diagonal come from points close to each other successively forward in time $((i,j), (i+l, j+l),\ldots,(i+T, j+T))$. Thus, a recurrent diagonal line indicates a stable recurrence of the phase relationship for a time interval corresponding to the length of the diagonal (T). The time interval separating different diagonals is the recurrence period. Recurrent points organized in rows and columns do not convey any information about the timing of the periodicity, since they are not successively forward in time.

In order to assess the organization of recurrence points into specific qualitative patterns, we used three particular descriptors of the plot features [16]. The first one is the Percent Recurrence (PR), calculated as the percent ratio between the number of recurrence points and the total number of points. It quantifies the percentage of the plot occupied by recurrence points, the more periodic the signal dynamics, the higher the PR value. The second variable is the Percent Determinism (PD) defined as the percent ratio between the number of the recurrence points forming diagonal lines longer than a fixed threshold (l) and the total number of recurrence points. This variable discriminates between spurious recurrent points and those with specific diagonal line organization and contains the information about the duration of a stable interaction: the longer the interactions, the higher the PD value. The third marker is the Entropy of Recurrence (ER), which is the Shannon entropy of the diagonal lengths distribution. After calculating the probability p_i of each upward diagonal length greater than the threshold value l, the Shannon entropy is obtained as follows:

$$\mathrm{ER} = -\sum p_i \log p_i \qquad (2)$$

ER quantifies the distribution of the recurrent points forming diagonals. Since RPs' upward diagonal lines suggest existing stable phase relationships between the signals, ER is an index of the deterministic structure of the dynamics, measured in binary (base 2) bits of information: the more deterministic structure of the RP, the smaller the number of bits requested to represent this structure.

Note that the choice of the threshold value l for the length of the diagonals is crucial for the correct estimation of both PD and ER. High values for l leads to an under-estimation of these parameters. Upon considerations on the frequencies of the analyzed time series, to obtain

a fair comparison of the different analyzed signals, we set the minimum duration of a stable recurrence to 2 s ($l = 4$ samples for the experimental data).

2.3. The Van Der Pol oscillator

In order to test how the proposed RPs descriptors work, we used the Van Der Pol model. It is described by the following non-linear differential second order equation [20]:

$$\ddot{x} + \varepsilon(x^2 - 1)\dot{x} + \omega_0^2 x = f(t) \quad (3)$$

$f(t)$ is the forcing term, and ε is a model parameter (it must be a positive constant). In the absence of forcing term, the Van der Pol oscillator exhibits periodic oscillations at ω_0, sustained by the non-linear term. When $f(t)$ is a periodic term, different kinds of interference occur between the forcing term $f(t)$ and the Van Der Pol oscillator $x(t)$, by varying the amplitude and frequency of the external stimulus. Although this model is not strictly interpretable from a physiological point of view, it well reproduces interaction phenomena observed in experimental data, such as sub-harmonic synchronization and full entrainment [20].

3. Results

3.1. Simulation results

By varying the amplitude and the frequency of the sinusoidal forcing term $f(t)$, we analyzed three coupling patterns between the forcing term and the Van der Pol oscillator: no interaction, sub-harmonic synchronization, and full entrainment (Fig. 1, upper part, panels A, B and C, respectively). Sub-harmonic synchronization can be obtained by setting the frequency of the sinusoidal forcing term close to twice ω_0 (self-oscillations). Full-entrainment was obtained by applying a forcing term with a relatively high amplitude.

Fig. 1 shows the RPs and the RQA results for each analyzed coupling pattern (middle part). The degrees of coupling of the three analyzed phenomena are correctly discriminated by the RQA (Fig. 1, lower part). Particularly, the increase of synchronization between signals, from no interaction to full entrainment, is marked by an increased number of recurrence points and of diagonals in the RPs, which give increased values of PR and PD. Conversely, ER decreases from no-interaction to full-entrainment. The higher the synchronization between the time series, the more

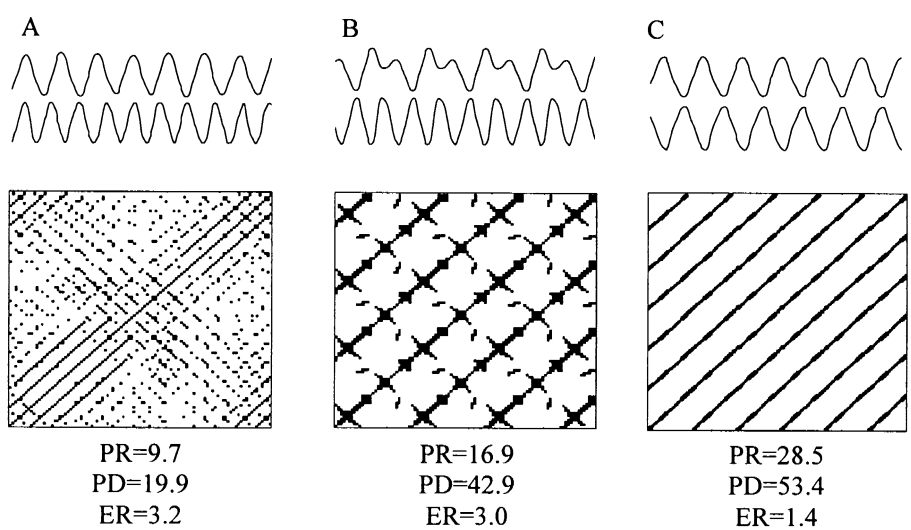

Fig. 1. Simulation results obtained with the Van der Pol oscillator. A: no interaction phenomena; B: sub-harmonic synchronization; C: full entrainment. Tracks of the forcing term and the oscillator (upper part), RPs (middle part), and RQA results (lower part).

deterministic their interaction, the smaller the ER value. ER is higher when the diagonals have different lengths, regardless the number of the diagonals themselves.

3.2. Experimental results

The spectral densities of both HRV and BPV signals (not shown) during 15 breaths per min stage are characterized in all subjects by an HF component centered at the respiratory frequency (0.25 Hz) and by an LF component which seems not to be influenced by the respiration (center frequency ranging 0.08-0.12 Hz).

During 12 breaths per min stage, (respiration frequency 0.2 Hz) the power spectra of both HRV and BPV series show, in eight subjects out of ten, an LF component clearly centered at half HF frequency (0.10 Hz).

During 8 breaths per min stage, in all subjects, only one component centered at the respiratory frequency (0.13 Hz) is visible both in HRV and BPV signals, LF and HF components cannot be distinguished any more and only a unique component at 0.13 Hz can be observed.

3.2.1. HRV-respiration

Fig. 2, panel A, shows the results obtained for the interaction between the HRV signal and the respiratory activity, in the three stages of the experimental protocol (15, 12 and 8 breaths per min, left, middle and right column, respectively), for one subject. About 100 s tracks of HRV and respiratory time series are reported, together with the corresponding RPs. Similar results have been obtained for all the other subjects. Note the increase of coupling between the two time series, from 15 to 8 breaths per min stage.

Table 1 summarizes the results averaged all over the population (mean $\pm$ standard deviation (S.D.)), also reported in Fig. 2, panel B: during 15 breaths per min stage, averaged RQA parameters are PR $= 14.8 \pm 4.2$, PD $= 24.5 \pm 4.8$, ER $= 4.2 \pm 0.13$; during 12 breaths per min, PR $= 24.3 \pm 3.5$, PD $= 62.3 \pm 9.2$, ER $= 3.6 \pm 0.2$; during 8 breaths per min stage, PR $= 27.2 \pm 3.5$, PD $= 68.7 \pm 6.2$ and ER $= 2.3 \pm 0.2$.

PR, PD and ER obtained during the 12 breaths per min stage result significantly different from those obtained during 15 breaths per min stage ($P < 0.00$l for PD and $P < 0.01$ for PR and ER, Wilcoxon's non-parametric test for paired data). PD and PR obtained during 12 breaths per min stage are lower than those obtained during 8 breaths per min stage, whereas ER is higher; in addition the difference of PD and ER values reaches a statistical significance ($P < 0.0$l for PD and $P < 0.001$ for ER). For the three RQA parameters, no overlapping is found between 8 and 15 breaths per min stages.

3.2.2. BPV-respiration

The results obtained for the interaction between the BPV signal and the respiratory activity, in the three stages of the experimental protocol (15, 12 and 8 breaths per min, left, middle and right panel, respectively) are shown in Fig. 3, panel A, for the same subject as in Fig. 2. As for the HRV signal, the BPV turns out to be fully synchronized with respiration during the 8 breaths per min stage. The RQA parameters averaged all over the population are (Table 2), during 15 breaths per min stage, PR $= 14.2 \pm 3.7$, PD $= 34.8 \pm 3.1$ and ER $= 4.3 \pm 0.4$; during 12 breaths per min RQA gave PR $= 16.2 \pm 5.2$, PD $= 56.3 \pm 6.3$, ER $= 3.9 \pm 0.2$; during 8 breaths per min stage, PR $= 17.9 \pm 2.9$, PD $= 62.3 \pm 9.1$ and ER $= 2.6 \pm 0.6$.

The differences between PD and ER values obtained during 15 and 12 breaths per min stages reach statistical significance ($P < 0.001$ for PD and $P < 0.01$ for ER), whereas the difference between PR values does not ($P = 0.1$). Concerning the differences of RQA parameters between 12 and 8 breaths per min stages, only ER results to be significantly different ($P < 0.001$) and there is no difference in PR and PD values ($P = 0.7$). Still, no overlapping is found for the three RQA parameters between 8 and 15 breaths per min stages.

4. Discussion

Although the ANS functionality has been extensively studied by means of spectral and cross-

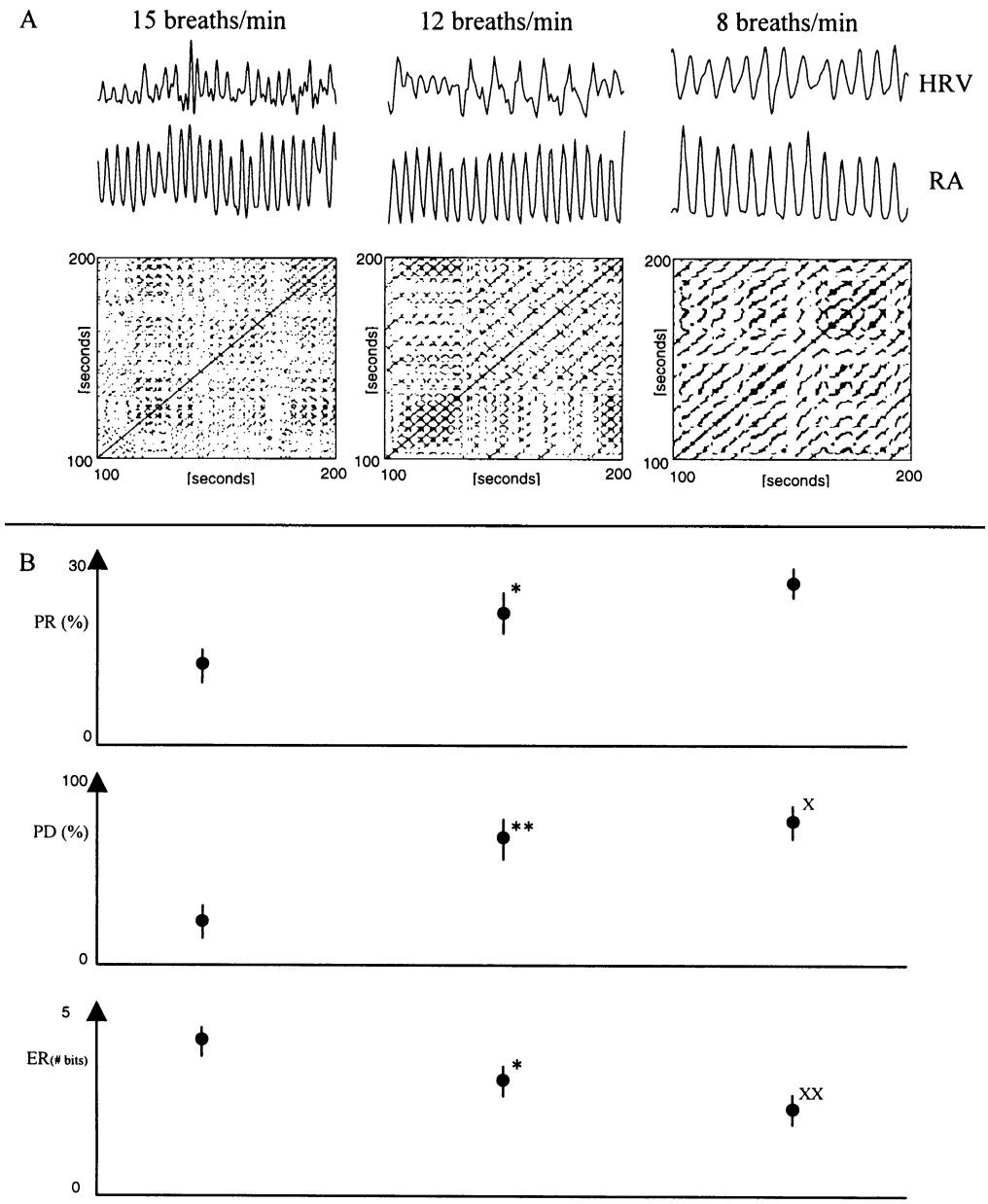

Fig. 2. (A) Experimental results obtained for one subject (15, 12 and 8 breaths per min, left, middle and right column, respectively). About 100-s tracks of HRV and respiratory time series are reported, together with the corresponding RPs. (B) PR, PD and ER values averaged all over the population (mean $\pm$ standard deviation, 15, 12 and 8 breaths/mm, left, middle and right column, respectively). $^{**}P < 0.00112$ versus 15 breaths per min; $^{*}P < 0.0112$ versus 15 breaths per min. $\sim\ \sim P < 0.0018$ versus 12 breaths per min; $\mathrm{X} \sim\ <_{0 \sim 01}$ 8 versus 12 breaths per min.

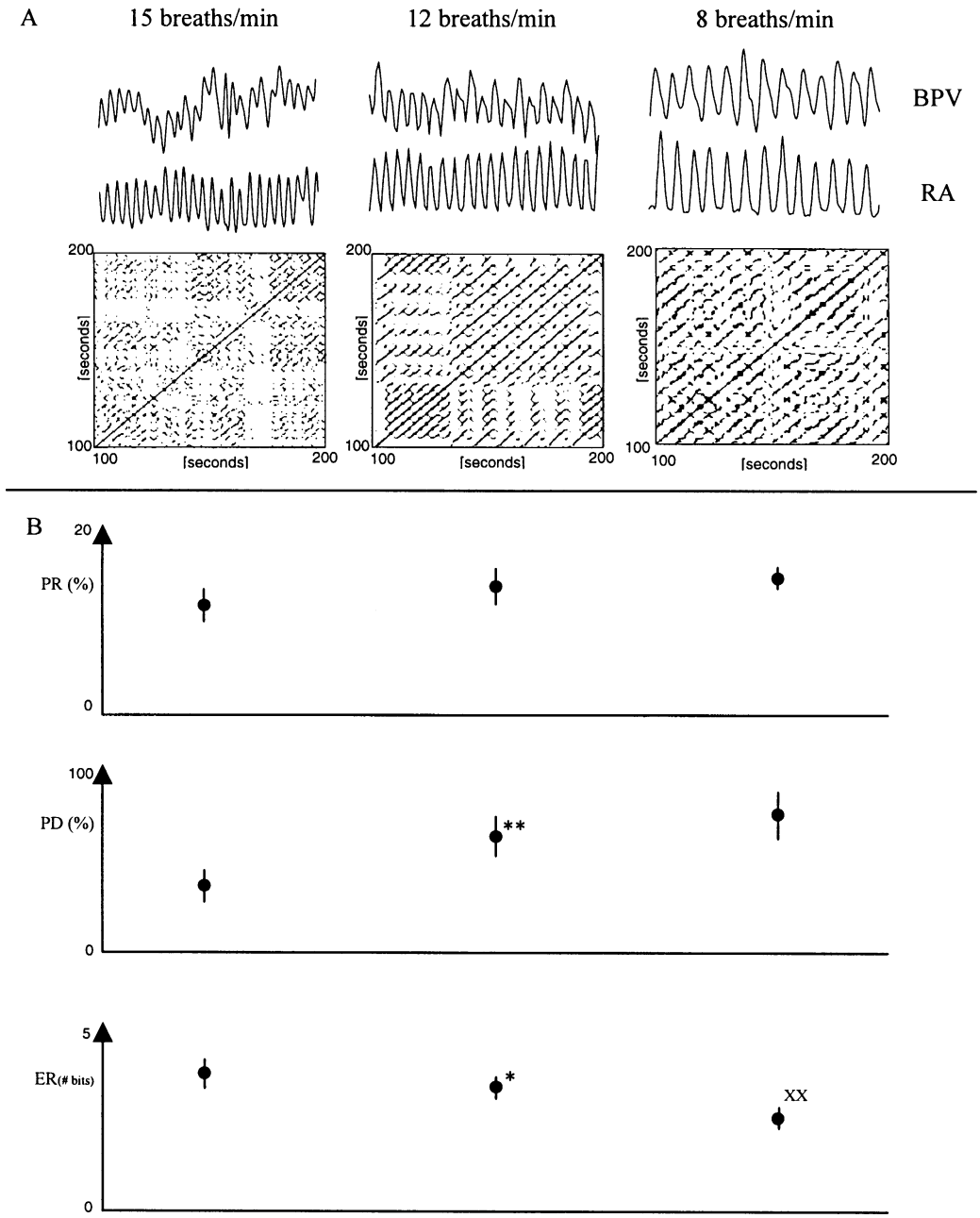

Fig. 3. (A) Experimental results obtained for one subject (15, 12 and 8 breaths per min, left, middle and right column, respectively). About 100-s tracks of BPV and respiratory time series are reported, together with the corresponding RPs. (B) PR, PD and ER values averaged all over the population (mean $\pm$ standard deviation, 15, 12 and 8 breaths per min, left, middle and right column, respectively). $^{**}P < 0.00112$ versus 15 breaths per min; $^{*}P < 0.0112$ versus 15 breaths per min. $^{XX}P < 0.0018$ versus 12 breaths per min.

spectral analysis of cardiovascular variability signals, non-linear dynamics have been recently shown to provide a relevant description of operation of this control system [11–13]. In addition, the interaction of breathing, heart rate and blood pressure are considered important for the understanding of the functional organization of the ANS [13].

We hereby proposed a new quantitative measurement of the degree of coupling between respiration and cardiovascular variability signals, based on the RQA. We estimated the degree of coupling by quantifying the spatio-temporal recurrent patterns of the interaction between the respiratory rhythm and the HR and BP variability series, in different breathing conditions.

We found different coupling patterns in the three stages of the experimental protocol, no interaction in the first stage (15 breaths per min), a kind of sub-harmonic synchronization in the second stage (12 breaths per min), and a full entrainment condition in the third one (8 breaths per min).

Spectral analysis showed that during 15 breaths per min the respiratory rhythm did not affect either HRV or BPV spontaneous fluctuations (but for the respiratory-induced fluctuations). During 12 breaths per min, we observed typical sub-harmonic synchronization patterns between the respiration and the cardiovascular variability signals (LF rhythm locked to the half of the respiratory frequency). The LF rhythm resulted to be fully entrained with the respiratory one, during the 8 breaths per min stage, in all the subjects. However, although spectral analysis detects shifting of the LF rhythm to the HF frequency all over the recording period, this linear tool considers the cardiovascular variability signal as a linear superposition of oscillations at different frequencies and can not quantify the degree of nonlinear coupling between different rhythms.

So far, RPs have been used to qualitatively detect transient phase locking patterns in the interaction between different oscillators [8,17]. Recently, it has been suggested their use to quantitatively estimate the degree of coupling among physiological oscillating sources [21]. Following this approach, we used the RQA approach to quantify the repetitive patterns of interaction between respiration and cardiovascular variability signals in a time-to-time domain. An observed recurrent pattern indicates that the (temporal) periodicity of one series has almost the same features as the other series. The number and the length distribution of the diagonals in a RP, measured by PD and ER, respectively, encode the deterministic features of the plot itself.

RQA turned out to be suitable for a quantitative evaluation of the observed coupling patterns among rhythms, both in simulated and real data, providing different degrees of coupling. The results from the simulated data showed that the increase of the degree of coupling between the signals was marked by the increase of PR and PD, and by the decrease of ER. When the RQA was applied to experimental data, PD and ER revealed to be the most significant variables, compared with PR; the better performance of these two variables can be explained by their low intrinsic sensitivity to spurious, isolated recurrent points, which may be introduced by random noise.

The three RQA parameters succeeded in discriminating the situation of no-interaction from the full-entrainment, for both the couples HRV-respiration and BPV-respiration. The sub-harmonic synchronization phenomena has been successfully distinguished from the situation of

Table 1
RQA results averaged all over the population (mean $\pm$ standard deviation), for the coupling between HRV and respiration

Stage	HRV-respiration		
	PR (mean $\pm$ standard deviation)	PD (mean $\pm$ standard deviation)	ER (mean $\pm$ standard deviation)
15 breaths per min	14.8 ± 4.2	24.5 ± 4.8	4.2 ± 0.13
12 breaths per min	24.3 ± 3.5	62.3 ± 9.2	3.6 ± 0.2
8 breaths per min	27.2 ± 3.5	68.7 ± 6.2	2.3 ± 0.2

Table 2
RQA results averaged all over the population (mean ± standard deviation), for the coupling between BPV and respiration

Stage	BPV-respiration		
	PR (mean ± standard deviation)	PD (mean ± standard deviation)	ER (mean ± standard deviation)
15 breaths per min	14.2 ± 3.7	34.8 ± 3.1	4.3 ± 0.4
12 breaths per min	16.2 ± 5.2	56.3 ± 6.3	3.9 ± 0.2
8 breaths per min	17.9 ± 2.9	62.3 ± 9.1	2.6 ± 0.6

no-interaction but only to a minor extent from that of full synchronization. A certain degree of non-linear coupling exists during the sub-harmonic synchronization phenomenon, significantly higher than that occurring when the LF rhythm seems not to be influenced by the respiratory rhythm. However, the sub-harmonic synchronization is not easily distinguishable from the full-entrainment condition, though generally weaker. It can be speculated that the sub-harmonic synchronization phenomenon is due to a non-linear mechanism somehow similar to that characterizing a full synchronization, but featuring a lower degree of non-linear coupling. Still, it should be noted that ER succeeded in distinguishing between sub-harmonic and full synchronization for both HRV and BPV, while PD did not. This result suggests that the difference between sub-harmonic and full synchronization phenomena can be better detected from the diagonal length distribution (encoded by ER) rather than from the number of diagonals (encoded by PD). Further, since a diagonal length represents the time duration of a recurrence, the two interaction phenomena differ for the duration of stable recurrences and only to a minor extent for their number (quantified by PD). However, the strongest coupling between respiration and cardiovascular variability signals occurs during the last stage of the experimental protocol (8 breaths per min), which elicits a full synchronization between the LF and the HF rhythms in the cardiovascular variability series.

From a physiological viewpoint, it is difficult to precisely identify the mechanisms responsible for the observed non-linear interaction. Our knowledge of the functional organization of the ANS is indeed still incomplete, given its complexity and the large number of involved physiological variables. Several mechanisms can be hypothesized to explain the non-linear coupling between respiratory and spontaneous rhythms of cardiovascular variability signals, such as changes in venous return induced by lung volume, a central coupling of cardiovascular and respiratory centers at the brain stem level [7,22], or central non-linear oscillating interacting sources (generating LF, HF and respiratory rhythms) influenced by forcing functions arising from physiologic control loops [7].

The ANS functionality has been already investigated by the RQA of single embedded time series of HRV and/or BPV. Dabire' et al. quantified the RP obtained from both HRV and BPV time series by using PR, PD and the longest diagonal, this latter inversely related to the Lyapunov exponent [23]. They showed that these non-linear indexes better reflected the sympathetic tone of BP and the parasympathetic tone of HR, than linear indexes derived from the spectral analysis. The longest diagonal of a RP has been also demonstrated to be a useful index to survey the autonomic function in diabetic subjects [24]. The variability of the cardiovascular signals is very complex and may reflect non-linear interaction between sympathetic and parasympathetic systems and between the cardiovascular and the respiratory systems. Our approach could provide important physiological information for the understanding of the neurovegetative coordination underlying normal and pathophysiologically disturbed behaviors. Obviously, the need to extend the method to a larger number of subjects as well as to the study of pathological situations is crucial. It could be interesting to test whether the non-linear mechanisms and the degrees of nonlin-

ear coupling obtained here can be reproduced in more patients, in different experimental conditions, in several patho-physiological conditions of clinical relevance, or in different variability signals.

5. Conclusions

In this investigation, we analyzed the interaction between cardiovascular and respiratory systems by means of a quantitative estimation of the degree of coupling based on the RQA. During the three stages of the experimental protocol, various types of synchronization phenomena, ranging from fully de-coupled to completely synchronized signals were observed and correctly discriminated. Higher degrees of non-linear coupling were found when the respiratory frequency was close to the LF rhythm, or almost twice the LF frequency. Weaker coupling was observed when the respiratory frequency was 0.25 Hz.

The possibility to quantify both linear and non-linear coupling between respiration and cardiovascular variability signals may provide a useful technique to assess the ANS functionality. Clinical application of our approach should focus on new experimental protocols, with the stimulation of one of the two ANS branches or the analysis of pathologies linked to the ANS.

References

[1] M.C. Mackey, L. Glass, Oscillation and chaos in physiological control systems, Science 197 (1977) 287–289.
[2] L. Glass, Cardiac arrhytmias and circle maps-A classical problems, Chaos 1 (1) (1991) 13–19.
[3] M.R. Guevara, L. Glass, A. Shrier, Phase locking, period-doubling biforcations, and irregular dynamics in periodically stimulated cardiac cells, Science 214 (1981) 1350–1352.
[4] S. Alkserod, Spectrum analysis of hearth rate fluctuation: a quantitative probe of beat-to-beat cardiovascular control, Science 213 (1981) 220–222.
[5] M. Pagani, F. Lombardi, S. Guzetti, O. Rimidli, R. Furlan, P. Pizzinelli, G. Sandrone, G. Malfatto, S. Dell'Orto, E. Piccaluga, M. Turiel, G. Baselli, S. Cerutti, A. Malliani, Power spectral analysis of a beat-to-beat heart rate and blood pressure variability as a possible marker of symphato–vagal interaction in man and conscious dog, Circ. Res. 59 (1986) 178–193.
[6] A. Malliani, M. Pagani, F. Lombardi, S. Cerutti, Cardiovascular neural regulation explored in the frequency domain, Circulation 84 (1991) 482–492.
[7] J.P. Saul, D.T. Kaplan, R. Kitney, Nonlinear interaction between respiration and heart rate: classical physiology or entrained nonlinear oscillators, IEEE Computers Cardiol. Proc. (1989) 209-302.
[8] A. Porta, G. Baselli, N. Montano, T. Gnecchi-Ruscone, F. Lombardi, A. Malliani, S. Cerutti, Non-linear dynamics in the beat-to-beat variability of sympathetic activity in decerebrate cats, Methods Inform. Med. 33 (1994) 89–93.
[9] D. Hoyer, D. Kaplan, M. Palus, B. Pompe, H. Seidel, New systems-analytical approaches to nonlinear coordination, IEEE Eng. Med. Biol. 17 (6) (1998) 58–61.
[10] D. Hoyer, O. Hader, U. Zwiener, Relative and intermittent cardiorespiratory coordination, IEEE Eng. Med. Biol. 16 (1) (1997) 97–104.
[11] D. Hoyer, B. Pompe, H. Herzel, U. Zwiener, Nonlinear coordination of cardiovascular autonomic control, IEEE Eng. Med. Biol. 17 (6) (1998) 17–21.
[12] D. Hoyer, D. Kaplan, F. Schaaff, M. Eiselt, Determinism in bivariate cardiorespiratory phase-space sets, IEEE Eng. Med. Biol. 17 (6) (1998) 26–31.
[13] D. Hoyer, R. Bauer, B. Walter, U. Zwiener, Estimation of non-linear couplings on the basis of complexity and predictability-a new method applied to cardiorespiratory coordination, IEEE Trans. BME 45 (1998) 1–8.
[14] B. Pompe, P. Blindh, D. Hoyer, M. Eiselt, Using mutual information to measure coupling in the cardiorespiratory system, IEEE Eng. Med. Biol. 17 (6) (1998) 32–39.
[15] J.P. Eckmann, S.O. Kamphorst, D. Ruelle, Recurrence plots of dynamical systems, Europhys. Lett. 4 (1987) 973–977.
[16] C.L. Webber, J.P. Zbilut, Dynamical assessment of physiological systems and states using recurrence plot strategies, J. Appl. Physiol. 76 (2) (1994) 965–973.
[17] A. Porta, G. Baselli, N. Montano, T. Gnecchi-Ruscone, F. Lombardi, A. Malliani, S. Cerutti, Classification of coupling patterns among spontaneous rhythms and ventilation in the sympathetic discharge of decerebrated cats, Biol. Cybern. 75 (1996) 163–172.
[18] G. Baselli, S. Cerutti, S. Civardi, D. Liberati, F. Lombardi, A. Malliani, M. Pagani, Spectral and cross-spectral analysis of heart rate and arterial blood pressure variability signals, Comput. Biomed. Res. 19 (6) (1986) 520–534.
[19] R.W. De Boer, J.M. Karemaker, J. Strackee, Comparing spectra of series of point elements particularly for heart rate variability data, IEEE Trans. BME 31 (1984) 384–387.
[20] N. Minorski, Non-Linear Oscillations, Van Nostrand, New York, 1962.
[21] F. Censi, V. Barbaro, P. Bartolini, G. Calcagnini, A. Michelucci, G.F. Gensini, S. Cerutti, Spatio-temporal recurrent patterns of atrial depolarization during atrial

fibrillation assessed by recurrence plot quantification, Ann. Biomed. Eng. 28 (1) (2000) 61–70.
[22] M.G. Rosenblurn, J. Kurths, A. Pikovsky, C. Schafer, P. Tass, H. Abel, Synchronization in noisy systems and cardiorespiratory interaction, IEEE Eng. Med. Biol. 17 (6) (1998) 46–53.
[23] H. Dabire', D. Mestivier, J. Jarnet, M.E. Safar, N.P. Chau, Quantification of sympathetic and parasympathetic tones by non-linear indexes in normotensive rats, Am. J Physiol. 275 (Heart Circ. Physiol. 44) (1998) H1290–H1297.
[24] D. Mestivier, N.P. Chau, X. Chanudet, B. Baudeceau, P. Larroque, Relationship between diabetic autonomic dysfunction and heath rate variability assessed by recurrence plot, Am. J. Physiol. 272 (Heart Circ. Physiol. 41) (1997) H1094–H1099.